Since January 2020 Elsevier has created a COVID-19 resource centre with free information in English and Mandarin on the novel coronavirus COVID-19. The COVID-19 resource centre is hosted on Elsevier Connect, the company's public news and information website.

Virology 546 (2020) 79–87

Contents lists available at ScienceDirect

Virology

journal homepage: www.elsevier.com/locate/virology

Aspartic acid at residue 185 modulates the capacity of HP-PRRSV nsp4 to antagonize IFN-I expression

Ze-yu Wei[a,b], Fang Liu[a,b], Yu Li[a,c], Hong-lei Wang[a,b], Zi-ding Zhang[a,c], Zhong-zhou Chen[a,d], Wen-hai Feng[a,b,*]

[a] State Key Laboratory of Agrobiotechnology, China
[b] Department of Microbiology and Immunology, College of Biological Sciences, China
[c] Department of Botany, College of Biological Sciences, China
[d] Department of Biochemistry and Molecular Biology, College of Biological Sciences, China Agricultural University, Beijing, 100193, China

ARTICLE INFO

Keywords:
PRRSV
nsp4
IFN-I
3C-like serine protease

ABSTRACT

In a previous study, we have shown that highly-pathogenic PRRSV (HP-PRRSV) nonstructural protein 4 (nsp4) antagonizes type I IFN expression induced by poly(I:C). Here, we demonstrated that the mutation of Aspartic acid 185 (Asp185) impaired the ability of nsp4 to inhibit IFN-I production induced by poly(I:C). Subsequently, we verified that all the mutants at the residue 185, regardless of amino acid size (including Cys and Ser) and charge (including Glu and Lys), impaired nsp4 catalytic activity. However, when Asp185 in nsp4 was replaced by a similar structure amino acid Asparagine 185 (Asn185), nsp4 stayed but with a decreased protease activity. Importantly, the recombinant virus with Asn185 mutation in HP-PRRSV-nsp4 exhibited slower replication rate and higher ability to induce IFN-I expression compared with wild-type (wt) HP-PRRSV.

1. Introduction

Porcine reproductive and respiratory syndrome (PRRS) caused by PRRS virus (PRRSV) continues to be a threat to the swine industry worldwide (Fang and Snijder, 2010). PRRSV belongs to the family *Arteriviridae*, which also includes equine arteritis virus (EAV), lactate dehydrogenase-elevating virus (LDV), simian hemorrhagic fever virus (SHFV), and the recently identified wobbly possum disease virus (WPDV) (Kuhn et al., 2016; Li et al., 2012). PRRS manifests itself clinically with severe reproductive failures in sows and respiratory distress in piglets (Chand et al., 2012; Albina, 1997). Specifically, the emergences of highly pathogenic PRRSV strains in China have posed a new threat to the swine industry (Tian et al., 2007a).

PRRSV is an enveloped positive-stranded RNA virus, and its genome is approximately 15.4 kb in length with at least 11 open reading frames (ORFs), including ORF1a, ORF1b, ORF2a, ORF2b, ORF3 to ORF7, ORF5a, and a transframe fusion [TF] ORF, which encode two polyprotein precursors (pp1a and pp1ab) and 8 structural proteins (Barrette-Ng et al., 2002; Dokland, 2010; Fang et al., 2012). The two polyproteins are subsequently cleaved into mature nonstructural proteins (nsps) by ORF1a-encoded proteases including nsp1α, nsp1β, nsp2, and nsp4 (Fang and Snijder, 2010; Snijder et al., 1995, 1996). Nsp1 and nsp2 are involved in the cleavage at nsp1/2 and nsp2/3 sites, respectively, while nsp4 is responsible for the cleavage of the remaining nsps (Ziebuhr et al., 2000; Snijder et al., 1992). Nsp4, a 3C-like serine protease (3CLSP), plays a significant role in the processing of pp1a and pp1ab to release nsp3 to nsp12 from pp1a/ab (van Aken et al., 2006a; Li et al., 2015).

Type I interferons (IFNs), the crucial antiviral cytokines, activate intracellular antimicrobial programs and influence the development of innate and adaptive immune responses (Ivashkiv and Donlin, 2014). During virus infection, the pattern-recognition receptors (PRRs) recognize specific pathogen-associated molecular patterns (PAMPs) to regulate the expression of IFNs through intracellular signaling cascades (Takeuchi and Akira, 2007; Tetreau et al., 2017). In these signaling pathways, NF-κB essential modulator (NEMO) and virus-induced signaling adapter (VISA, also called MAVS or IPS-1) play essential roles in regulating the expression of IFN-I and inflammatory cytokines (Kawai et al., 2005; Satoshi and Shizuo, 2006; Akira et al., 2006).

Viruses have developed strategies, including defensive mechanisms to inhibit IFN-I production, to evade and subvert host immune response throughout evolution (Bowie and Unterholzner, 2008). Previous reports have demonstrated that PRRSV expresses some IFN-I antagonists such as the nsp1, nsp4, and nsp11 to suppress IFN-I production (Luo et al., 2008; Huang et al., 2014, 2016; Shi et al., 2010, 2011; Music and Gagnon, 2010). We have previously shown that HP-PRRSV-nsp4

* Corresponding author. State Key Laboratory of Agrobiotechnology, China.
E-mail address: whfeng@cau.edu.cn (W.-h. Feng).

https://doi.org/10.1016/j.virol.2020.04.007
Received 12 February 2020; Received in revised form 8 April 2020; Accepted 9 April 2020
Available online 21 April 2020

inhibits IFN-I production induced by poly(I:C) dependent on the 3CLSP activity of nsp4 (Huang et al., 2014). Previous studies have mainly focused on the nsp4 catalytic triad and there are rare studies about the functions of other amino acids in nsp4 (Huang et al., 2014, 2016; Chen et al., 2019). However, when there is a deletion mutation instead of the catalytic triad, nsp4 also loses its ability to inhibit IFN-I production induced by poly(I:C) (Huang et al., 2014). Given the pivotal role of nsp4 in regulating IFN-I and the fact that there are still unknown functions of nsp4, it is necessary for us to study this 3CLSP at the amino acid level.

Here, we demonstrated that the residue Asp at position 185 in nsp4 played a role in modulating the capacity of highly-pathogenic PRRSV to antagonize IFN-I expression. The finding showed that nsp4 with mutations replacing Asp185 impaired its 3CLSP activity of cleaving VISA and NEMO to regulate IFN-I expression. Subsequently, we found that amino acids structure of residue 185 in nsp4 regulated its 3CLSP activity. Importantly, we showed that the recombinant virus HP-PRRSV-D185N replicated much more slowly and had lower ability to cause cytopathic effects *in vitro*.

2. Results

2.1. Amino acid at residue 185 modulates the capacity of nsp4 to inhibit the induction of IFN-I

Previous studies have shown that HP-PRRSV-nsp4 inhibits IFN-I production induced by poly(I:C) and the catalytic triad His39-Asp64-Ser118 is essential for nsp4 to block IFN-β production. As a 3C-like serine protease, nsp4 has three domains (called domain I, II, and III, respectively) and the catalytic triad is located in domain I and domain II (Tian et al., 2009). To investigate if there is any other amino acids in nsp4 in addition to His39-Asp64-Ser118 that are important for nsp4 to inhibit IFN-I production, we generated several nsp4 mutants with point amino acid substitution by Alanine (Ala). Alignments for most of the highly pathogenic PRRSV strains showed that the mutated amino acids were relatively conserved in domain I to III (data not shown). CRL-2843 cells were co-transfected with each of the plasmids encoding these mutants and an IFN-β-luciferase reporter plasmid. At 24 h post-transfection, cells were treated with poly(I:C) for 8 h and luciferase activities were examined. As shown in Fig. 1A, wild-type (wt) nsp4 strongly inhibited poly(I:C)-induced IFN-β promoter activation, while Alanine185 (Ala185) mutation in nsp4 disrupted its ability to inhibit IFN-β promoter activation. To see if the mutations had effects on nsp4 expression, we did Western blot. As shown in Fig. 1A, the nsp4 mutants expressed the same as wt-nsp4. The Isoleucine178 (Ile178) and Aspartic acid185 (Asp185) are located in domain III in nsp4, while the other mutants are located in domain I and domain II, respectively. Interestingly, multiple sequence alignments of the 3CLSPs of the viruses in the family *Arteriviridae*, including both highly pathogenic PRRSV and classical PRRSV strains and EAV, showed that Asp185 was highly conserved (Fig. 1B). To exclude the possibility that the amount of nsp4-D185A might play a role, we did a dose-dependent experiment. Our results indicated that nsp4-D185A did not inhibit the poly(I:C)-induced IFN-β promoter activity even at higher doses (Fig. 1C). Then, we confirmed this result by analyzing IFN-β expression. As shown in Fig. 1D, wt nsp4 significantly suppressed IFN-β expression to 54%, while nsp4 with Ala185 mutation did not inhibit IFN-β expression induced by poly(I:C) (Fig. 1D). Taken together, these data show that Asp185 plays a role in modulating the capacity of HP-PRRSV-nsp4 to antagonize IFN-I expression.

2.2. Nsp4 with mutation in Asp185 has impaired capacity for cleaving NEMO and VISA

Considering that VISA plays a pivotal role in RLRs (RIG I like receptors) signaling and NEMO is required for the signaling in the canonical NF-κB pathway, PRRSV has evolved mechanisms to manipulate these crucial molecules to counteract the production of type I IFNs (Kawai et al., 2005; Huang et al., 2014, 2016; Hayden and Ghosh, 2008). To investigate whether Asp185 is important for nsp4 to cleave VISA and NEMO, wt nsp4 and nsp4-D185A plasmids were transfected into CRL-2843 cells, respectively. Western blot results showed that wt nsp4 cleaved VISA and NEMO, while nsp4-D185A did not (Fig. 2A and B). To further investigate whether Asp185 also plays a role in modulating typical PRRSV-nsp4 to cleave VISA and NEMO, we transfected VR2332-nsp4 and VR2332-nsp4-D185A into CRL-2843 cells, respectively. Our results confirmed the same phenomenon by using nsp4 from the typical PRRSV strain VR2332 (Fig. 2C and D). Collectively, these data demonstrate that Asp185 regulates the capacity of nsp4 to cleave VISA and NEMO.

2.3. The structure of residue Asp185 in nsp4 might play a role in keeping its 3CLSP activity

Nsp4 is a 3C-like serine protease, which is responsible for most of the nonstructural protein processing including nsp3′4 and nsp11′12 in PRRSV replication (Tian et al., 2009). We then investigated whether the protease activity alteration in nsp4 was associated with Asp185 mutation. To verify the 3CLSP activity of nsp4, we first generated fusion proteins nsp3′4(S118Y) and nsp11′12, which were used as substrates (Huang et al., 2014; Xu et al., 2010). The nsp3′4(S118Y) substrate contains the last 8 amino acids of nsp3 and the whole amino acids of nsp4, which has a mutated Ser118 to disrupt its 3CLSP activity to avoid self-cleaving. The nsp11′12 substrate contains the whole amino acids of both nsp11 and nsp12. As expected, nsp4 with Ala185 mutation did not cleave the substrates, implying that replacing Asp185 with Ala impaired its protease activities (Fig. 3A and B). To further clarify how residue Asp185 regulates the 3CLSP activity, we first generated a nsp4 mutant (nsp4-D185E) by replacing Asp185 with a negatively charged amino acid Glutamate185 (Glu, E) or a mutant (nsp4-D185K) by replacing Asp185 with a positively charged amino acid Lysine185 (Lys, K). We then transfected each of the vectors into HeLa cells along with nsp11′12 expression plasmids. As shown in Fig. 3C, both nsp4-D185E and nsp4-D185K did not cleave nsp11′12, suggesting that the charge of the residue 185 is not a key factor in affecting the protease activity of nsp4. Next, to explore if the size of residue 185 in nsp4 plays a role in regulating its 3CLSP activity, we made nsp4 mutants with Serine185 (Ser, S) and Cysteine185 (Cys, C), which have similar sizes with aspartic acid. Similarly, nsp4-D185C and nsp4-D185S did not cleave nsp11′12 (Fig. 3D), implying that the amino acid size of residue 185 in nsp4 is also not a key factor in keeping its protease activity. Then, to investigate whether the residue structure at position 185 in nsp4 plays a role in keeping its protease activity, we replaced nsp4 Asp185 with Asparagine (Asn, N), which has the most similar structure to aspartic acid among the other 19 amino acids. Surprisingly, nsp4-D185N cleaved nsp11′12 (Fig. 3E), even though the cleaving was in a less effective way, suggesting that the residue structure of Asp185 in nsp4 might play an important role in keeping its protease activity.

2.4. Nsp4 with Asn185 substitution reduces its protease activity

Considering that nsp4-D185N can cleave the optimal substrates, we next performed experiments to examine the proteolytic activity of nsp4-D185N *in vitro*. Previous study shows that pET32a-nsp3'4(S118Y) is used as one of the most optimal substrates (Xu et al., 2010). Once the substrate is cleaved at the nsp3 and nsp4(S118Y) junction (E/G) by the active 3CLSP, pET32a-Nsp3 moiety of 18 kDa will be expected. To investigate the nsp4 proteolytic activity, purified wt nsp4 and nsp4-D185N with substrates were incubated in Tris-HCl buffer for 12 h. SDS-PAGE results showed that there were more cleaved products by wt nsp4 than nsp4-D185N (Fig. 4A). To further confirm this result, a fluorogenic peptide substrate containing the cleavage sites (E/G) derived from nsp11′12 was synthesized, and then fluorescence resonance energy transfer (FRET) assay was performed to explore whether wt nsp4 and

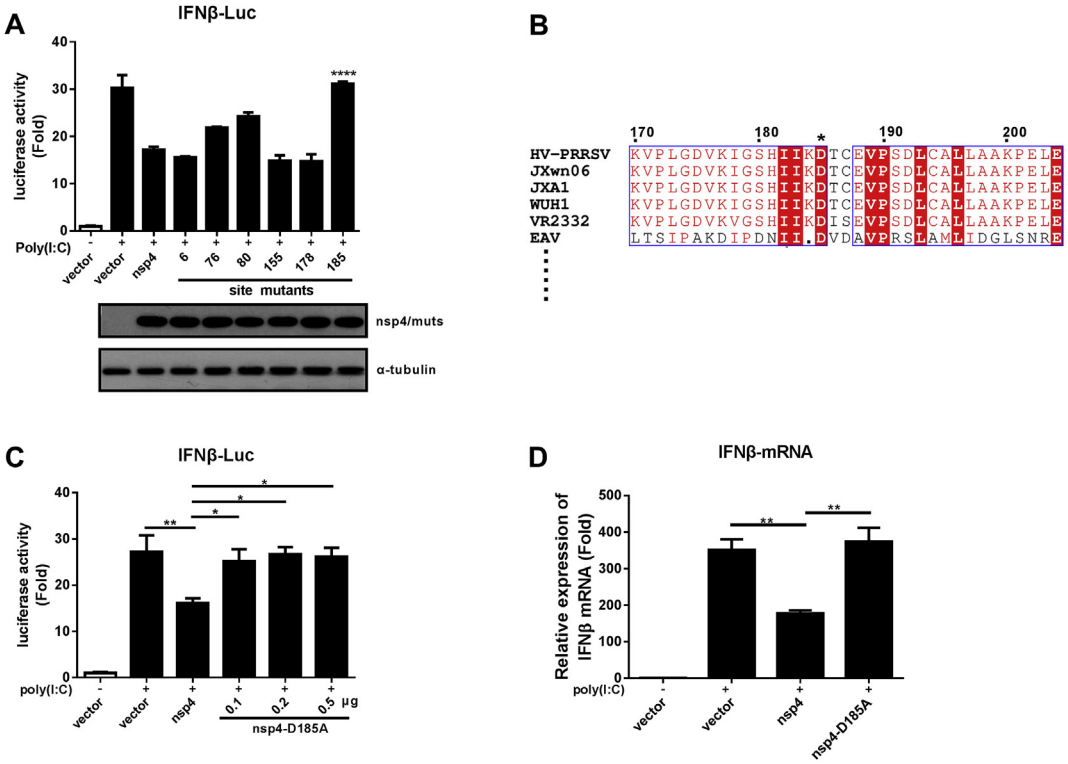

Fig. 1. Amino acid Asp at position 185 modulates the capacity of nsp4 to inhibit the activation of IFN-β. (A) CRL-2843 cells were co-transfected with pGL3-IFN-β-Luc, pRL-TK, and wt nsp4 or mutant expression plasmids. pRL-TK was used as an internal control for transfection efficiency. At 24 h post transfection, cells were stimulated with or without poly(I:C) (10 μg/ml). Luciferase assays were performed 8 h after the stimulation. In addition, lysates of cells were subjected to Western blot analysis with antibodies against nsp4 to show the protein expression. (B) Multiple sequence alignment of the 3CLSPs (aa170-aa204) of the viral members in the family *Arteriviridae*. Asp185 was indicated by asterisk. The arterivirus nsp4 amino acids were from HV (GenBank accession number JX317648.1), JXwn06 (GenBank accession number EF641008.1), JXA1 (GenBank accession number EF112445.1), WUH1 (GenBank accession number EU187484.1), VR2332 (GenBank accession number EF536003.1) and EAV (GenBank accession number X53459.3). (C) Nsp4-D185A expression plasmids at different doses (0.1, 0.2, and 0.5 μg) were co-transfected into CRL-2843 cells with pGL3-IFN-β-Luc and pRL-TK. At 24 h post transfection, cells were treated with or without poly(I:C) (10 μg/ml) for 8 h and then analyzed for luciferase activities. (D) CRL-2843 cells were transfected with control vector, wt nsp4, or nsp4-D185A expression plasmid. Cells were treated with or without poly(I:C) (10 μg/ml) for 2 h, and IFN-β expression was analyzed using qPCR. The structure-based sequence alignment was generated using the ESPript website (http://espript.ibcp.fr/ESPript/ESPript/index.php). Data are means ± SD from three independent experiments. Differences were evaluated by *Student's t-test.**, $P < 0.05$; **, $P < 0.01$; ***, $P < 0.001$.

nsp4-D185N cleave the peptide substrates with different proteolytic activity. As shown in Fig. 4B, the fluorescence value with wt nsp4 had a sharping increase along with time. However, the fluorescence value with nsp4-D185N increased slowly and lightly. In addition, when a small amount of purified proteins were incubated with sufficient fluorogenic peptide substrates *in vitro*, the fluorescence value with wt nsp4 was significantly higher than that with nsp4-D185N after 10 min reaction (Fig. 4C). These results suggest that replacing aspartic acid with asparagine at position 185 reduces the proteolytic activity of nsp4.

2.5. Recombinant HP-PRRSV with Asn185 mutation in nsp4 replicates less efficiently in vitro

To investigate whether Asn185 mutation in nsp4 has an effect on HP-PRRSV replication, we generated a recombinant HP-PRRSV (named as PRRSV-D185N) by replacing wt nsp4 with nsp4-D185N in HP-PRRSV strain HV (Fig. 5A). We then infected PAMs with wt HP-PRRSV strain HV and the recombinant virus PRRSV-D185N at an MOI of 0.01. As shown in Fig. 5B, there were hardly any living PAMs existed at 48 h post-infection (hpi) with wt HV, while there were no obvious cytopathic effects observed in PAMs infected with PRRSV-D185N. In addition, PRRSV-D185N grew much slower than wt HV, with a titer about 100 times lower than that of wt HV at 48 hpi (Fig. 5C). Next, we investigated whether wt HV and PRRSV-D185N had different abilities to induce IFN-I expression. PAMs were infected with either wt HV or PRRSV-D185N, and then harvested for IFN-I expression analysis. At 8 hpi, IFN-α and IFN-β expression induced by PRRSV-D185N increased about 4 folds and 3 folds higher than that induced by wt HV, respectively (Fig. 5D). To study whether PRRSV-D185N has less ability to inhibit poly(I:C)-induced type I IFNs, we infected PAMs at an MOI of 0.01 and then stimulated the cells with poly(I:C) at 24 hpi. At 6 h post-stimulation, the mRNA levels of type I IFNs were analyzed using qPCR. As shown in Fig. 5E, wt HV down-regulated IFN-α expression to 10%, while PRRSV-D185N reduced IFN-α expression to 33%. Wt HV down-regulated IFN-β expression to 31% and PRRSV-D185N reduced IFN-β expression to 76%. Similar results were obtained with the analysis of ISGs (Fig. 5F). Taken together, these data indicate that the recombinant virus PRRSV-D185N has a less effective replication rate and much more potential to induce type I IFNs expression *in vitro*.

3. Discussion

In the present study, we demonstrated that the residue Asp185 modulates the capacity of highly-pathogenic PRRSV nsp4 to antagonize IFN-I expression. Our data showed that nsp4 with Ala185 mutation had impaired ability in cleaving VISA and NEMO. We further verified that residue structure of Asp185 in nsp4 might play a role in keeping its 3CLSP activity. Importantly, we demonstrated that the recombinant virus PRRSV-D185N with Asn185 mutation in nsp4 had a lower replication rate and higher ability to induce type I IFNs expression compared with its parental HP-PRRSV HV strain *in vitro*.

Although PRRSV is sensitive to IFNs, it evolves a series of

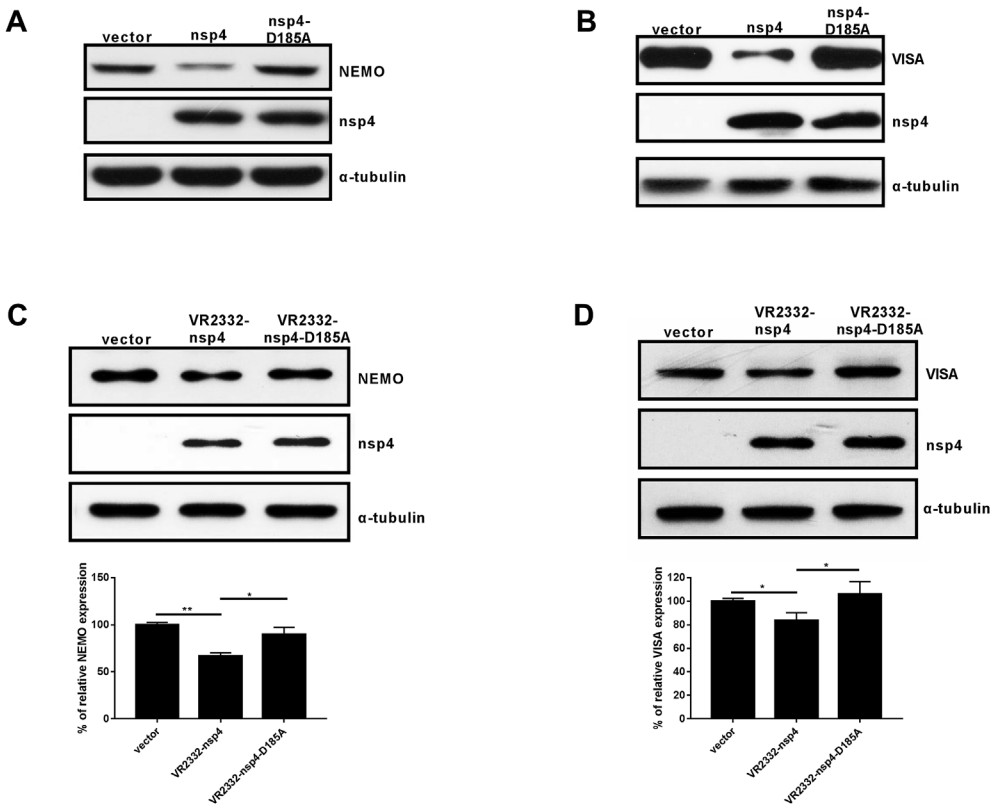

Fig. 2. Amino acid Asp at position 185 has impact on nsp4 to cleave NEMO and VISA. (A and B) CRL-2843 cells were transfected with wt HV-nsp4 and HV-nsp4-D185A expression plasmids, respectively. At 24 h post transfection, Western blot analysis was performed to detect NEMO (A), VISA (B) and nsp4. (C and D) VR2332-nsp4 and VR2332-nsp4-D185A expression plasmids were transfected into CRL-2843 cells. At 24 h post-transfection, cells were harvested to analyze NEMO (C), VISA (D) and nsp4 by Western blot. The density of the bands in the figure was quantified by densitometry scanning.

mechanisms to counteract type I IFNs. Tao et al. has found that PRRSV nsp4 can cleave pDCP1a to down-regulate pDCP1a expression, which is an ISG and inhibits PRRSV replication (Tao et al., 2018). Chen et al. has determined that the amino acid at residue 155 in PRRSV nsp4 contributes to its inhibitory effect on IFN-β transcription *in vitro* by altering its subcellular distribution (Chen et al., 2014). In our study, we characterized 6 nsp4 mutants with amino acid point mutations conserved in the domain I to III in most of the highly pathogenic PRRSV

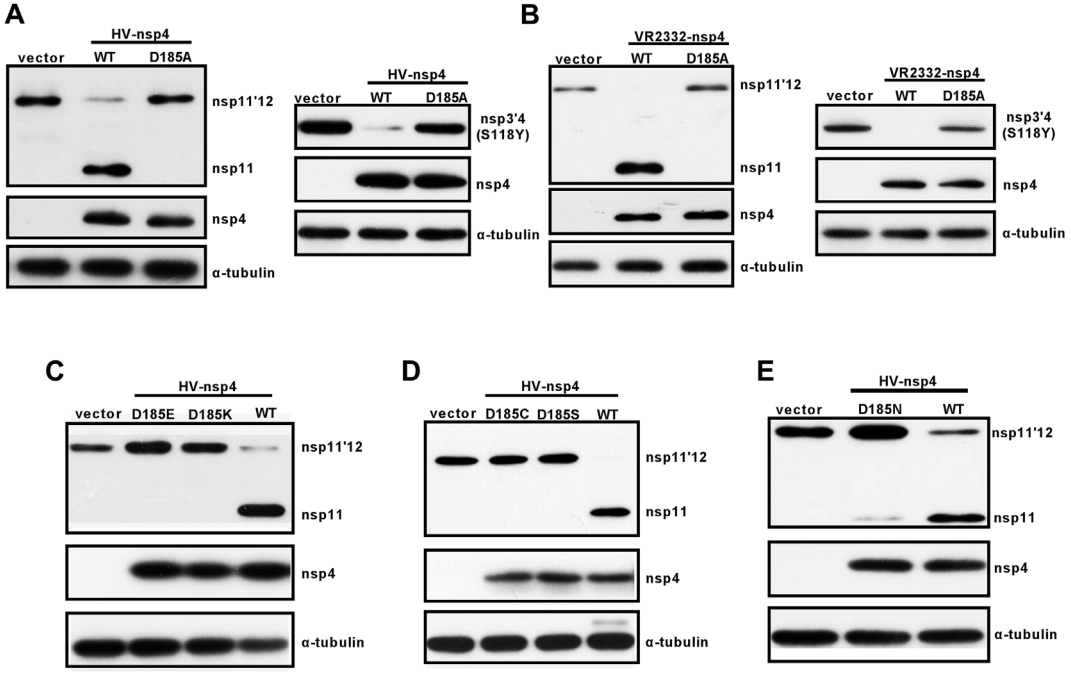

Fig. 3. The residue structure of Asp185 might be important for nsp4 to keep its protease catalytic activity. (A and B) Flag-tagged nsp11'12 and nsp3'4(S118Y) fusion protein expression plasmids were co-transfected into HeLa cells with plasmids encoding HV-nsp4 and HV-nsp4-D185A (A), and VR2332-nsp4 and VR2332-nsp4-D185A (B), respectively. Cell lysates were analyzed by Western blot with antibodies specific for Flag and c-Myc (for nsp4). α-tubulin was used as a loading control. (C–E) HeLa cells were co-transfected with nsp11'12 fusion protein and nsp4 mutant expression plasmids, including nsp4-D185E and nsp4-D185K (C), nsp4-D185C and nsp4-D185S (D), and nsp4-D185N (E). At 24 h later, cells were harvested. Western blot analysis for nsp11'12 and nsp4 expression was performed by using antibodies against Flag and c-Myc, respectively.

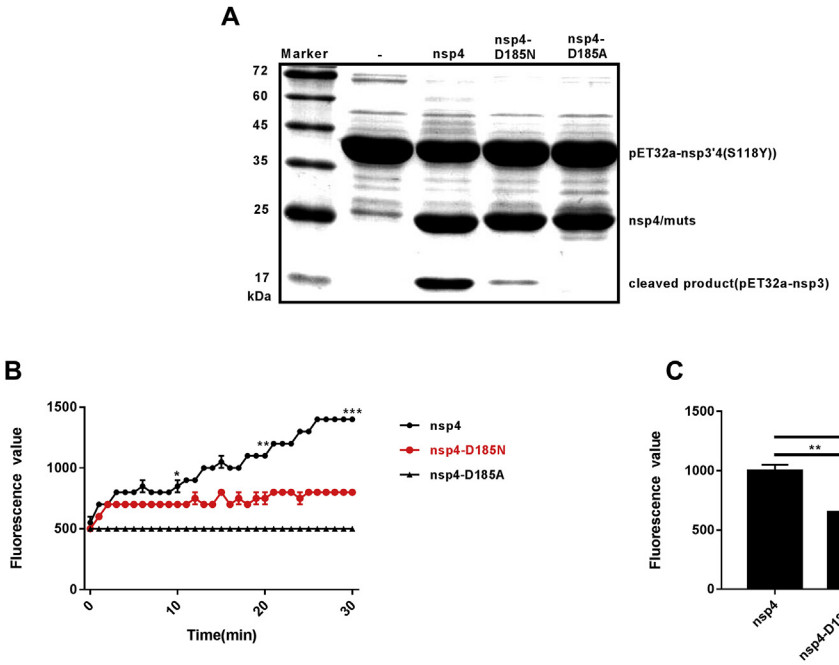

Fig. 4. Wt nsp4 and nsp4-D185N cleave substrates with different proteolytic activities *in vitro*. (A) The enzyme (5 mM) and substrate (7 mM) were incubated for 12 h at 4 ˚C in buffers introduced in methods. (B and C) Fluorogenic peptide substrates were incubated with wt nsp4 and nsp4-D185N, respectively. Fluorogenic signals were collected per minute. Significance in 10 min, 20 min and 30 min was shown (B). Fluorogenic signals were collected after 10 min incubation (C). Data are means ± SD from three independent experiments. Differences were evaluated by *Student's t-test*. *, $P < 0.05$; **, $P < 0.01$; ***, $P < 0.001$.

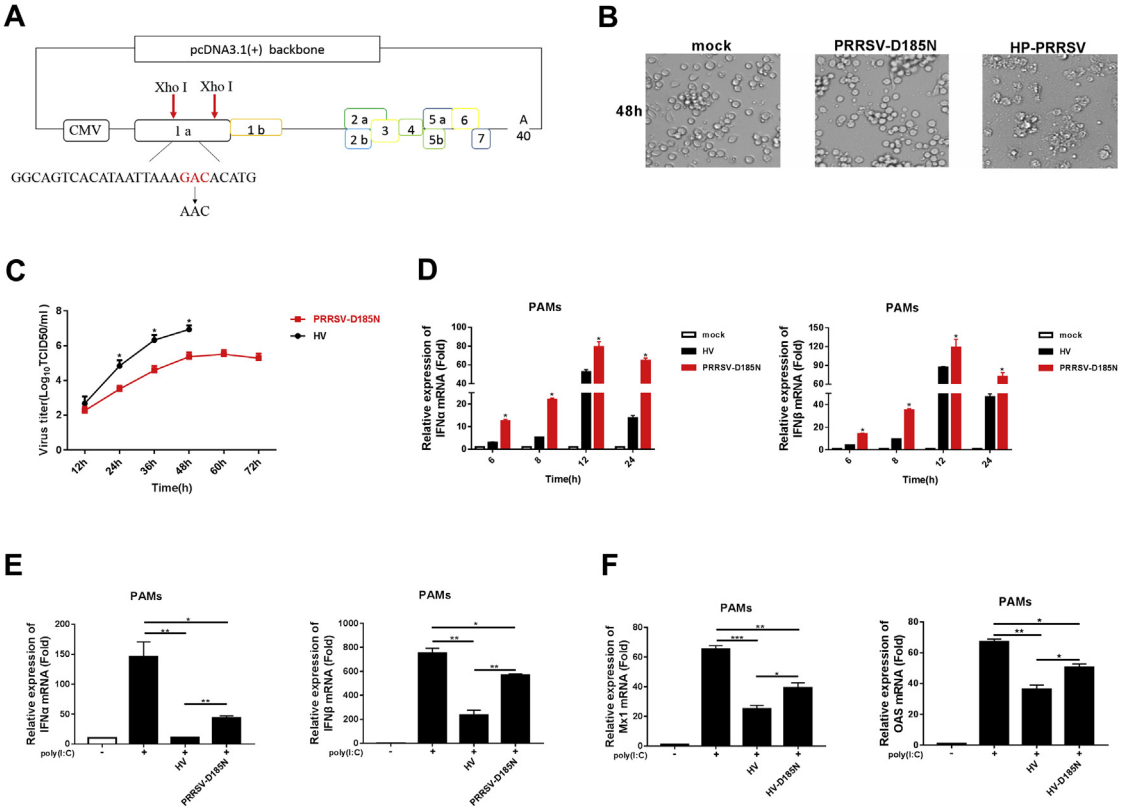

Fig. 5. Recombinant virus PRRSV-D185N grows significantly slower than its parental wild-type HP-PRRSV HV *in vitro*. (A) Strategy for the construction of the recombinant PRRSV-D185N. The restriction enzyme cutting sites and mutation site were indicated. (B–D) PAMs were infected with either HP-PRRSV HV or the recombinant virus PRRSV-D185N at an MOI of 0.01. (B) Representative images of cytopathic effects induced by PRRSV at 48 hpi. (C) Supernatants were harvested at the indicated times and titrated for virus titer using the $TCID_{50}$ method. (D) At 6, 8, 12, and 24 hpi, total RNAs were extracted from cells, and qPCR was performed to analyze the expression of IFN-α and IFN-β, respectively. (E and F) Cells were treated with poly(I:C) (10 μg/ml) for 6 h or left untreated at 24 h post PRRSV infection. qPCR was performed to analyze the expression of IFN-α and IFN-β (E), and Mx1 and OAS (F). GAPDH was used as an internal control. Data are means ± SD from three independent experiments. Differences were evaluated by *Student's t-test*.*, $P < 0.05$; **, $P < 0.01$; ***, $P < 0.001$.

strains. We found that Asp185 mutation in nsp4 disrupted its ability to suppress IFN-β promoter activity induced by poly(I:C) (Fig. 1A and C). Considering that Asp185 in nsp4 is strongly conserved not only in HP-PRRSV strains but also in other viruses of the family *Arteriviridae*, we speculate that Asp185 in nsp4 might contribute to its 3CLSP activity (Fig. 1B).

Like other RNA viruses in the order *Nidovirales*, such as EAV and severe acute respiratory syndrome coronavirus (SARS-CoV), PRRSV-encoded proteases play a prominent role in virus replication. PRRSV nsp4 is responsible for most of the nonstructural protein processing to join into the virus replication (Aeksiri and Jantafong, 2017). PRRSV nsp4 has three domains, including two antiparallel β-barrels (called domain I and domain II, respectively) and an extra C-terminal α/β domain (domain III) (Tian et al., 2009). A canonical catalytic triad composed of Ser118, His39, and Asp64 has been documented in the open cleft between domain I and domain II. However, our previous study shows that nsp4 without domain III has an impaired ability to inhibit IFN-β, suggesting that domain III is also important in keeping nsp4 activity (Huang et al., 2014). Even though limited studies suggest that domain III plays a role in nsp4 protease processing (van Aken et al., 2006b), there are still a lot of mysteries about it. Here, we demonstrated that Asp185 mutation in nsp4 impaired its ability to cleave nsp3′4(S118Y) and nsp11′12 (Fig. 3A and B). Interestingly, we observed that both of HV nsp4-D185A and VR2332 nsp4-D185A still cleaved some nsp3′4, but not nsp11′12. We speculate that it might be due to the specific structure of this nsp3′4(S118Y) substrate. Although both nsp3′4(S118Y) and nsp11′12 are substrates for nsp4, the amino acids in nsp3′4(S118Y) are totally different from nsp11′12. Nsp4-D185A might have some protease activity for nsp3′4 but not for nsp11′12. However, the underlying rationale needs to be investigated in the future.

Previous studies have found that several residue mutations in 3C-like protease can change its enzymatic activity to influence the protease function. As for SARS-CoV 3C-like protease, mutating residues Ser284, Thr285 and Ile286 located in domain III of the 3C-like protease to Ala causes a super-active triple-mutant STI/A with activity enhancement (Shi and Song, 2006; Yang et al., 2003). In our study, Asp185 also locates in the domain III of nsp4, which is spatially far from the catalytic triad. After a series of attempts to illustrate the impact of Asp185 on nsp4, we found that only the Asn185 mutation still kept the proteolytic activity of nsp4. Although Asp has negatively charged side chains while Asn does not, both of them are hydrophilic. Structure of Asn is the most similar one to that of Asp, because the structure of amide group (-$CONH_2$) is similar to carboxyl group (-COOH) and both of them have carbon chains with the same length. These suggest that it is the residue structure itself but not the charge and residue size at position 185 that might regulate its proteolytic activity (Fig. 3C–E). To investigate how the residue structure plays the role, we compared the side chain structures of the residues (Fig. 6A). Analysis showed that there were hydrogen bonds between Asp185 and Leucine159 (Leu159) and between Asp185 and Ser160 (Fig. 6B). However, when Asp185 was replaced by Ala, there were no hydrogen bonds formed between Ala185 and Leu159 or Ser160 (Fig. 6C). Interestingly, when Asp185 was replaced with Asn, similar hydrogen bonds were formed between Asn185 and Leu159 and between Asn185 and Ser160 (Fig. 6D). Energy analysis showed that nsp4 with Ala185 mutation had higher energy value than nsp4 with Asp185 or Asn185 mutation, indicating that both Asp185 and Asn185 can keep nsp4 at a stable condition (data not show). These findings suggest that the hydrogen bonds between these residues might be an important factor in keeping nsp4 structure stable and its proteolytic activity. However, we are not sure if there are any changes caused by the mutation of Asp185 in nsp4 when it is combined with the substrates, since there is no published structure of *arterivirus* nsp4 in complex with its substrates.

Because the viral 3C-like proteases play an essential role in *arterivirus* replication, they have received much more attention as potential key antiviral targets including the development of attenuated vaccine and drugs. A previous report shows that the compounds targeting 3CLSP are used to identify inhibitors that suppress PRRSV replication (Chen et al., 2010). Danny van Aken et al. replace Ala155 and Asp156 in EAV nsp4 with Glycine (Gly) individually or both and get two impaired but not dead virus phenotypes (van Aken et al., 2006b). Since nsp4-D185N has impotent but not null proteolytic activities, it gives us a reason to construct the recombinant virus PRRSV-D185N. The recombinant PRRSV-D185N replicated significantly slower than wt HP-PRRSV HV in PAMs with a much lower titer *in vitro* (Fig. 5B and C). This is in consistent with the proteolytic activity study, which shows that the proteolytic activity of nsp4 with Asn185 mutation is decreased (Fig. 4A–C). Undoubtedly, PRRSV-D185N has a stronger ability to induce IFN-I, but relatively poor capacity to inhibit IFN-I production induced by poly(I:C) when compared with wt HP-PRRSV (Fig. 5D–F). The decreased replication rate and increased expression of IFN-I during PRRSV-D185N infection might contribute to the fact that the recombinant virus causes fewer obvious cytopathic effects *in vitro*. However, further studies need to be done to assess whether PRRSV-D185N is attenuated *in vivo*.

In conclusion, we have identified that Asp185 modulates the capacity of HP-PRRSV nsp4 to antagonize IFN-I production. We further show that it might be the residue structure at position 185 but not the residue size or charge that plays an important role in regulating nsp4 activity. Importantly, the recombinant PRRSV-D185N replicates less effectively when compared with its wt HP-PRRSV HV *in vitro*. These findings may provide some insights into the mechanisms about how nsp4 help PRRSV evade host innate immunity.

4. Materials and methods

Cells and viruses. CRL-2843 cells, a porcine alveolar macrophage cell line, were maintained in RPMI 1640 (Gibco) supplemented with 10% fetal bovine serum (FBS) (Gibco, Australia). HeLa and HEK293T cells were cultured in Dulbecco's minimum essential medium (DMEM) supplemented with 10% FBS. Porcine alveolar macrophages (PAMs) were obtained by postmortem lung lavage of 8-week-old specific-pathogen-free (SPF) pigs and maintained in RPMI 1640 with 10% FBS. All of the cells were cultured and maintained at 37 °C with 5% CO_2. HP-PRRSV strain HV (GenBank accession no. JX317648.1) was propagated and titrated on PAMs.

Antibodies and reagents. Antibody against NEMO (also known as IKKγ) was from Cell Signaling Technology. Rabbit anti-VISA (also known as MAVS, polyclonal antibody raised against residues 1–13 of MAVS) antibody was obtained from Abcam. Anti-α-tubulin antibody and anti-c-Myc antibody were purchased from MBL International Corporation. Anti-Flag antibody was from Sigma. Antibodies against histone 3 were purchased from Santa Cruz. Goat anti-mouse or anti-rabbit IgG secondary antibodies were also purchased from Santa Cruz. The antibody for PRRSV-nsp4 was prepared by our lab. Poly(I:C) was from InvivoGen.

Plasmids. Porcine IFNβ-luciferase reporter plasmid was constructed using pGL3-Basic vector as described elsewhere (Huang et al., 2014). pRL-TK containing the Renilla luciferase was used as a normalization control. The protein expression plasmid pCMV-HV-nsp4 has been described previously (Ma et al., 2013). To construct plasmid pCMV-VR2332-nsp4, nsp4 fragment of PRRSV strain VR2332 cDNA was cloned into the pCMV-Myc vector at EcoRI and XhoI sites. The Q5® Site-Directed Mutagenesis Kit was used to generate the point mutations including pCMV-HV-nsp4 mutants (D185A, D185E, D185K, D185C, D185S, and D185N) and pCMV-VR2332-nsp4-D185A. The nsp3'4(S118Y), which contains only the last 8 amino acids of nsp3 and S118Y mutation of nsp4, and the full length of nsp11'12 were cloned into the PRK5-flag vector at BamH I and Hind III sites. All the primers are listed in Table 1.

Luciferase reporter assays. CRL-2843 cells were seeded in 24-well

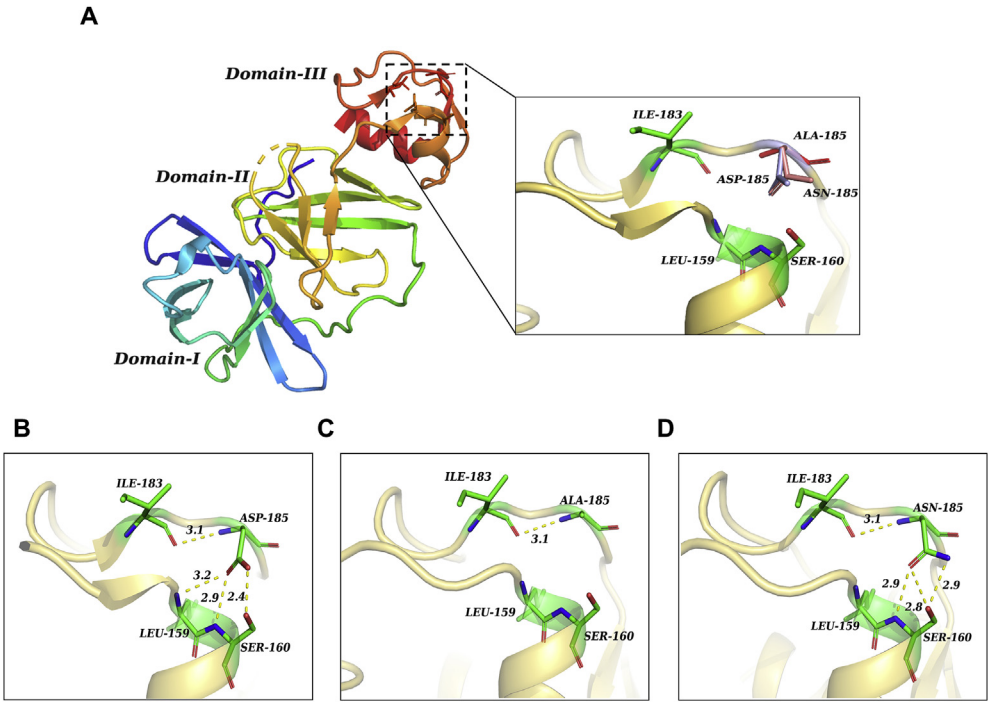

Fig. 6. Cartoon representation of the structure at residue 185 of PRRSV-nsp4. (A) Ribbon diagrams of the crystal structures of PRRSV nsp4 (PDB accession code 3FAN). Superposition of the residue 185 in wt PRRSV-nsp4 and nsp4 mutants. Asp185 was in light blue, Ala185 was in red, and Asn185 was in salmon. (B–D) Comparison of the hydrogen bonds formed between residue 185 and other residues in wt nsp4 (Asp185, (B)) and its mutants (Ala185 (C) and Asn185 (D)). Yellow broken lines indicated hydrogen bonds. Residues of 185 were labeled. Figures were generated using Pymol.

Table 1
Primers used for cloning mutations in nsp4.

Primer	Sequence(5′-3′)
VR2332-nsp4-F	ATGGGTGCCTTCAGAACTCG
VR2332-nsp4-R	TCATTCCAGTTCAGGTTTGGCAGC
HV-nsp4-D185A-F	CATAATTAAAGCTACATGCGAGG
HV-nsp4-D185E-F	CATAATTAAAGAGACATGCGAGG
HV-nsp4-D185K–F	CATAATTAAAAAGACATGCGAGG
HV-nsp4-D185C–F	CATAATTAAATGCACATGCGAGG
HV-nsp4-D185S–F	CATAATTAAATCGACATGCGAGG
HV-nsp4-D185N–F	CATAATTAAAAATACATGCGAGG
HV-nsp4-D185(AEKCSN)-R	TGACTGCCAATTTTCACATC
nsp3'4(S118Y)–F	ATGAGCGATAAAATTATTC
nsp3'4(S118Y)-R	TTCCAGTTCGGGTTTGGCAGC

Table 2
Primers used for real-time PCR.

Primer	Sequence(5′-3′)
IFN-β-F	AGCACTGGCTGGAATGAAAC
IFN-β-R	TCCAGGATTGTCTCCAGGTC
IFN-α-F	CTGCTGCCTGGAATGAGAGCC
IFN-α-R	TGACACAGGCTTCCAGGTCCC
Mx1-F	CACAGAACTGCCAAGTCCAA
Mx1-R	GCAGTACACGATCTGCTCCA
GAPDH-F	CCTTCCGTGTCCCTACTGCCAAC
GAPDH-R	GACGCCTGCTTCACCACCTTCT
OAS-F	AGCAAGGAAGCAGGAAAACA
OAS-R	GCTTCCCAGAAGATGCAAAG

plates at a cell density of 4 × 10^4 cells per well. At 12 h after plating, cells were transfected with the control plasmid or plasmids expressing nsp4 as well as mutants of nsp4 along with pGL3-IFN-β-Luc, and pRL-TK using jetPRIME™ (Polyplus). pRL-TK plasmid was used as a control for transfection efficiency. The total amount of DNA was kept constant by adding vector control plasmid. At 24 h post transfection, cells were treated with poly(I:C) for 8 h or left untreated. Cell extracts were prepared and analyzed for firefly and Renilla luciferase activities using the dual-luciferase reporter assay kit (Promega) according to the manufacturer's instructions.

RNA isolation and quantitative real-time PCR (qPCR). RNA isolation and qPCR were performed as described previously (Guo et al., 2013). PAMs were infected with HV-PRRSV or PRRSV-D185N for 6–24 h, and then treated with or without poly(I:C) (10 μg/ml) for 6 h. CRL-2843 cells were transfected with a control plasmid or plasmids expressing nsp4 or nsp4-D185A. At 24 h after transfection, cells were treated with poly(I:C) for 2 h or left untreated. Total RNAs were extracted with TRIzol (Invitrogen) and used for cDNA synthesis using the HiFiScript cDNA Synthesis Kit according to the manufacturer's instructions (Cwbiotech). Quantitative RT-PCR (qPCR) analysis was performed using FastSYBR Mixture with ROX (Cwbiotech) on the ViiATM7 real-time PCR System (Applied Biosystems). Gene-specific primers for IFN-β, IFN-α, Mx1, OAS, and GAPDH were designed and listed in Table 2. The expression of IFN-β, IFN-α, Mx1, and OAS was normalized to glyceraldehyde-3-phosphate dehydrogenase (GAPDH) and presented as fold induction relative to the control.

Western blot analysis. Cells were harvested and lysed in RIPA lysis buffer (Beyotime) with 100 U proteinase cocktail (Cwbiotech). Protein levels in each sample were quantified with the BCA assay kit (Pierce Biotechnology, Inc.). Similar amounts of proteins from each extract were resolved by SDS-PAGE and transferred to PVDF membranes (Millipore). Membranes were blocked with 5% nonfat milk in phosphate-buffered saline with 0.05% Tween 20 (PBST) for 30 min and then incubated for 2 h at room temperature with antibodies at a suitable dilution as recommended (anti-NEMO, -VISA and -histone 3 at 1:1000; anti-Flag, -α-tubulin, and -c-Myc at 1:2000; anti-nsp4 at 1:4000). The membranes were then incubated with the appropriate secondary antibody for 1 h at a dilution of 1:10,000. The antibodies were visualized by use of the ECL reagent according to the manufacturer's protocols.

Protein expression and purification. For wt nsp4 and the mutated nsp4 protein preparation, the recombinant plasmids were transformed into *E. coli* BL21 (DE3). And then, the transformed *E. coli* BL21 (DE3) grew at 37 °C in LB medium. Isopropyl-β-D-thiogalactopyranoside (IPTG) (0.5 mM) was added to the culture medium to induce the protein expression until the optical density at 600 nm (OD600) reached 0.6 to 0.8. Cells were collected after incubation at 18 °C for 8 h. PRRSV nsp4 expression and purification were carried out as described previously (Xu et al., 2010; Tian et al., 2007b).

Assays for enzymatic activities *in vitro*. A fluorescence-based

assay with the fluorogenic peptide substrate Dabsyl-KTAYFQLE↓GRHFE-Edans (95% purity, Beijing Scilight Biotechnology LLC.) was used to assess the activity of the nsp4 as well as nsp4-D185N (Tian et al., 2009). This peptide substrate contains the nsp11'nsp12 cleavage site (indicated by the arrow). The enhanced fluorescence due to the cleavage of the substrate by the enzyme was monitored at 490 nm with excitation at 340 nm (Matayoshi et al., 1990). The experiments were performed in a buffer consisting of 20 mM Tris–HCl (pH 7.3), 100 mM NaCl, 1 mM ethylenediaminetetraacetic acid, and 5 mM DTT. The measurements were done at 25 °C. The reaction was initiated by adding proteinase (final concentration, 5 μM) to the solution containing the fluorogenic peptide (500 μM) and monitored per minute to record the fluorescence value, or proteinase (5 μM) and fluorogenic peptide (50 μM) were incubated for 10 min and then the fluorescence value was recorded. As for proteolytic reaction, the proteolytic enzyme (5 mM) and substrate (7 mM) were incubated in 50 μl buffer mentioned above for 12 h at 4 °C. The reaction was stopped by the addition of a quarter volume of 5 × sample buffer. The proteins were analyzed using 15% (v/v) SDS-PAGE. The data of fluorogenic value were expressed as the average values of three replicate experiments.

Construction of the recombinant HP-PRRSV. The plasmid containing the assembled genome of HV (pcDNA3.1-HV) was constructed in our Lab (Wang et al., 2014). The full genome of HV is divided into two fragments, the long fragment and the short fragment. The short fragment contains the nsp4-coding region. The Q5® Site-Directed Mutagenesis Kit was used to generate the point mutation D185N within the short fragment. And then, the mutated fragment was inserted into the pcDNA3.1-HV fragment that was digested by XhoI restriction enzymes using HiFi DNA Assembly Master Mix (NEB) to generate the full-length infectious cDNA clones. The plasmid (pcDNA3.1-PRRSV-D185N) was then transfected into HEK293T cells. After 72 h post-transfection, cell culture supernatants were harvested and inoculated on PAMs and immunofluorescence assay was performed for virus detection (Wang et al., 2011). The rescued virus was designated as PRRSV-D185N. The viral titer was determined by the Reed-Muench method and expressed as 50% tissue culture infective doses ($TCID_{50}$)/ml.

Hydrogen bonds modeling. The structure of PRRSV-nsp4 (PDB accession number 3FAN) with residue 185 mutations was generated by the FoldX program. The figures of hydrogen bond distributions between residue 185 and Leu159 or Ser160 were generated by the Pymol program.

Statistical analysis. Statistical analysis was performed using Graphpad Prism software, and differences were analyzed using student's *t-test*. Significance was denoted as follows: $*p \leq 0.05$, $**p \leq 0.01$, $***p \leq 0.001$, and ns (not significant).

CRediT authorship contribution statement

Ze-yu Wei: Writing - original draft, Formal analysis, Data curation. **Fang Liu:** Formal analysis. **Yu Li:** Formal analysis. **Hong-lei Wang:** Formal analysis. **Zi-ding Zhang:** Supervision. **Zhong-zhou Chen:** Supervision. **Wen-hai Feng:** Writing - original draft, Supervision, Formal analysis.

Declaration of competing interest

The authors declared that no competing interests exist.

Acknowledgements

This work was supported by the National Natural Science Foundation of China (Grant No. 31572516), the National Natural Science Foundation of China (Grant No. 31630076), and National Key R &D Program of China (Grant No. 2017YFD0500601-1).

Appendix A. Supplementary data

Supplementary data to this article can be found online at https://doi.org/10.1016/j.virol.2020.04.007.

References

Aeksiri, N., Jantafong, T., 2017. Structural insights into type I and type II of nsp4 porcine reproductive and respiratory syndrome virus (nsp4 PRRSV) by molecular dynamics simulations. J. Mol. Graph. Model. 74, 125–134.
Akira, S., Uematsu, S., Takeuchi, O., 2006. Pathogen recognition and innate immunity. Cell 124, 783–801.
Albina, E., 1997. Epidemiology of porcine reproductive and respiratory syndrome (PRRS): an overview. Vet. Microbiol. 55, 309–316.
Barrette-Ng, I.H., Ng, K.K., Mark, B.L., Van Aken, D., Cherney, M.M., Garen, C., Kolodenko, Y., Gorbalenya, A.E., Snijder, E.J., James, M.N., 2002. Structure of arterivirus nsp4. The smallest chymotrypsin-like proteinase with an alpha/beta C-terminal extension and alternate conformations of the oxyanion hole. J. Biol. Chem. 277, 39960–39966.
Bowie, A.G., Unterholzner, L., 2008. Viral evasion and subversion of pattern-recognition receptor signalling. Nat. Rev. Immunol. 8, 911–922.
Chand, R.J., Trible, B.R., Rowland, R.R., 2012. Pathogenesis of porcine reproductive and respiratory syndrome virus. Curr Opin Virol 2, 256–263.
Chen, Z., Lawson, S., Sun, Z., Zhou, X., Guan, X., Christopher-Hennings, J., Nelson, E.A., Fang, Y., 2010. Identification of two auto-cleavage products of nonstructural protein 1 (nsp1) in porcine reproductive and respiratory syndrome virus infected cells: nsp1 function as interferon antagonist. Virology 398, 87–97.
Chen, Z., Li, M., He, Q., Du, J., Zhou, L., Ge, X., Guo, X., Yang, H., 2014. The amino acid at residue 155 in nonstructural protein 4 of porcine reproductive and respiratory syndrome virus contributes to its inhibitory effect for interferon-beta transcription in vitro. Virus Res. 189, 226–234.
Chen, J., Wang, D., Sun, Z., Gao, L., Zhu, X., Guo, J., Xu, S., Fang, L., Li, K., Xiao, S., 2019. Arterivirus nsp4 antagonizes interferon beta production by proteolytically cleaving NEMO at multiple sites. J. Virol. 93.
Dokland, T., 2010. The structural biology of PRRSV. Virus Res. 154, 86–97.
Fang, Y., Snijder, E.J., 2010. The PRRSV replicase: exploring the multifunctionality of an intriguing set of nonstructural proteins. Virus Res. 154, 61–76.
Fang, Y., Treffers, E.E., Li, Y., Tas, A., Sun, Z., van der Meer, Y., de Ru, A.H., van Veelen, P.A., Atkins, J.F., Snijder, E.J., Firth, A.E., 2012. Efficient -2 frameshifting by mammalian ribosomes to synthesize an additional arterivirus protein. Proc. Natl. Acad. Sci. U. S. A. 109, E2920–E2928.
Guo, X.K., Zhang, Q., Gao, L., Li, N., Chen, X.X., Feng, W.H., 2013. Increasing expression of microRNA 181 inhibits porcine reproductive and respiratory syndrome virus replication and has implications for controlling virus infection. J. Virol. 87, 1159–1171.
Hayden, M.S., Ghosh, S., 2008. Shared principles in NF-kappaB signaling. Cell 132, 344–362.
Huang, C., Zhang, Q., Guo, X.K., Yu, Z.B., Xu, A.T., Tang, J., Feng, W.H., 2014. Porcine reproductive and respiratory syndrome virus nonstructural protein 4 antagonizes beta interferon expression by targeting the NF-kappaB essential modulator. J. Virol. 88, 10934–10945.
Huang, C., Du, Y., Yu, Z., Zhang, Q., Liu, Y., Tang, J., Shi, J., Feng, W.H., 2016. Highly pathogenic porcine reproductive and respiratory syndrome virus Nsp4 cleaves VISA to impair antiviral responses mediated by RIG-I-like receptors. Sci. Rep. 6, 28497.
Ivashkiv, L.B., Donlin, L.T., 2014. Regulation of type I interferon responses. Nat. Rev. Immunol. 14, 36–49.
Kawai, T., Takahashi, K., Sato, S., Coban, C., Kumar, H., Kato, H., Ishii, K.J., Takeuchi, O., Akira, S., 2005. IPS-1, an adaptor triggering RIG-I- and Mda5-mediated type I interferon induction. Nat. Immunol. 6, 981–988.
Kuhn, J.H., Lauck, M., Bailey, A.L., Shchetinin, A.M., Vishnevskaya, T.V., Bao, Y., Ng, T.F., LeBreton, M., Schneider, B.S., Gillis, A., Tamoufe, U., Diffo Jle, D., Takuo, J.M., Kondov, N.O., Coffey, L.L., Wolfe, N.D., Delwart, E., Clawson, A.N., Postnikova, E., Bollinger, L., Lackemeyer, M.G., Radoshitzky, S.R., Palacios, G., Wada, J., Shevtsova, Z.V., Jahrling, P.B., Lapin, B.A., Deriabin, P.G., Dunowska, M., Alkhovsky, S.V., Rogers, J., Friedrich, T.C., O'Connor, D.H., Goldberg, T.L., 2016. Reorganization and expansion of the nidoviral family Arteriviridae. Arch. Virol. 161, 755–768.
Li, Y., Tas, A., Snijder, E.J., Fang, Y., 2012. Identification of porcine reproductive and respiratory syndrome virus ORF1a-encoded non-structural proteins in virus-infected cells. J. Gen. Virol. 93, 829–839.
Li, Y., Tas, A., Sun, Z., Snijder, E.J., Fang, Y., 2015. Proteolytic processing of the porcine reproductive and respiratory syndrome virus replicase. Virus Res. 202, 48–59.
Luo, R., Xiao, S., Jiang, Y., Jin, H., Wang, D., Liu, M., Chen, H., Fang, L., 2008. Porcine reproductive and respiratory syndrome virus (PRRSV) suppresses interferon-beta production by interfering with the RIG-I signaling pathway. Mol. Immunol. 45, 2839–2846.
Ma, Z., Wang, Y., Zhao, H., Xu, A.T., Wang, Y., Tang, J., Feng, W.H., 2013. Porcine reproductive and respiratory syndrome virus nonstructural protein 4 induces apoptosis dependent on its 3C-like serine protease activity. PloS One 8, e69387.
Matayoshi, E.D., Wang, G.T., Krafft, G.A., Erickson, J., 1990. Novel fluorogenic substrates for assaying retroviral proteases by resonance energy transfer. Science 247, 954–958.
Music, N., Gagnon, C.A., 2010. The role of porcine reproductive and respiratory syndrome (PRRS) virus structural and non-structural proteins in virus pathogenesis. Anim. Health Res. Rev. 11, 135–163.
Satoshi, U., Shizuo, A.J.U., 2006. Innate Immune Recognition of Viral Infection, vol. 56. pp. 1–8.

Shi, J., Song, J., 2006. The catalysis of the SARS 3C-like protease is under extensive regulation by its extra domain. FEBS J. 273, 1035–1045.
Shi, X., Wang, L., Zhi, Y., Xing, G., Zhao, D., Deng, R., Zhang, G., 2010. Porcine reproductive and respiratory syndrome virus (PRRSV) could be sensed by professional beta interferon-producing system and had mechanisms to inhibit this action in MARC-145 cells. Virus Res. 153, 151–156.
Shi, X., Wang, L., Li, X., Zhang, G., Guo, J., Zhao, D., Chai, S., Deng, R., 2011. Endoribonuclease activities of porcine reproductive and respiratory syndrome virus nsp11 was essential for nsp11 to inhibit IFN-beta induction. Mol. Immunol. 48, 1568–1572.
Snijder, E.J., Wassenaar, A.L., Spaan, W.J., 1992. The 5' end of the equine arteritis virus replicase gene encodes a papainlike cysteine protease. J. Virol. 66, 7040–7048.
Snijder, E.J., Wassenaar, A.L., Spaan, W.J., Gorbalenya, A.E., 1995. The arterivirus Nsp2 protease. An unusual cysteine protease with primary structure similarities to both papain-like and chymotrypsin-like proteases. J. Biol. Chem. 270, 16671–16676.
Snijder, E.J., Wassenaar, A.L., van Dinten, L.C., Spaan, W.J., Gorbalenya, A.E., 1996. The arterivirus nsp4 protease is the prototype of a novel group of chymotrypsin-like enzymes, the 3C-like serine proteases. J. Biol. Chem. 271, 4864–4871.
Takeuchi, O., Akira, S., 2007. [Pathogen recognition by innate immunity]. Arerugi 56, 558–562.
Tao, R., Fang, L., Bai, D., Ke, W., Zhou, Y., Wang, D., Xiao, S., 2018. Porcine reproductive and respiratory syndrome virus nonstructural protein 4 cleaves porcine DCP1a to attenuate its antiviral activity. J. Immunol. 201, 2345–2353.
Tetreau, G., Pinaud, S., Portet, A., Galinier, R., Gourbal, B., Duval, D., 2017. Specific pathogen recognition by multiple innate immune sensors in an invertebrate. Front. Immunol. 8, 1249.
Tian, K., Yu, X., Zhao, T., Feng, Y., Cao, Z., Wang, C., Hu, Y., Chen, X., Hu, D., Tian, X., Liu, D., Zhang, S., Deng, X., Ding, Y., Yang, L., Zhang, Y., Xiao, H., Qiao, M., Wang, B., Hou, L., Wang, X., Yang, X., Kang, L., Sun, M., Jin, P., Wang, S., Kitamura, Y., Yan, J., Gao, G.F., 2007a. Emergence of fatal PRRSV variants: unparalleled outbreaks of atypical PRRS in China and molecular dissection of the unique hallmark. PloS One 2, e526.
Tian, X., Feng, Y., Zhao, T., Peng, H., Yan, J., Qi, J., Jiang, F., Tian, K., Gao, F., 2007b. Molecular cloning, expression, purification and crystallographic analysis of PRRSV 3CL protease. Acta Crystallogr Sect F Struct Biol Cryst Commun 63, 720–722.
Tian, X., Lu, G., Gao, F., Peng, H., Feng, Y., Ma, G., Bartlam, M., Tian, K., Yan, J., Hilgenfeld, R., Gao, G.F., 2009. Structure and cleavage specificity of the chymotrypsin-like serine protease (3CLSP/nsp4) of Porcine Reproductive and Respiratory Syndrome Virus (PRRSV). J. Mol. Biol. 392, 977–993.
van Aken, D., Zevenhoven-Dobbe, J., Gorbalenya, A.E., Snijder, E.J., 2006a. Proteolytic maturation of replicase polyprotein pp1a by the nsp4 main proteinase is essential for equine arteritis virus replication and includes internal cleavage of nsp7. J. Gen. Virol. 87, 3473–3482.
van Aken, D., Snijder, E.J., Gorbalenya, A.E., 2006b. Mutagenesis analysis of the nsp4 main proteinase reveals determinants of arterivirus replicase polyprotein autoprocessing. J. Virol. 80, 3428–3437.
Wang, L., Zhang, H., Suo, X., Zheng, S., Feng, W.H., 2011. Increase of CD163 but not sialoadhesin on cultured peripheral blood monocytes is coordinated with enhanced susceptibility to porcine reproductive and respiratory syndrome virus infection. Vet. Immunol. Immunopathol. 141, 209–220.
Wang, L., Hou, J., Gao, L., Guo, X.K., Yu, Z., Zhu, Y., Liu, Y., Tang, J., Zhang, H., Feng, W.H., 2014. Attenuation of highly pathogenic porcine reproductive and respiratory syndrome virus by inserting an additional transcription unit. Vaccine 32, 5740–5748.
Xu, A.T., Zhou, Y.J., Li, G.X., Yu, H., Yan, L.P., Tong, G.Z., 2010. Characterization of the biochemical properties and identification of amino acids forming the catalytic center of 3C-like proteinase of porcine reproductive and respiratory syndrome virus. Biotechnol. Lett. 32, 1905–1910.
Yang, H., Yang, M., Ding, Y., Liu, Y., Lou, Z., Zhou, Z., Sun, L., Mo, L., Ye, S., Pang, H., Gao, G.F., Anand, K., Bartlam, M., Hilgenfeld, R., Rao, Z., 2003. The crystal structures of severe acute respiratory syndrome virus main protease and its complex with an inhibitor. Proc. Natl. Acad. Sci. U. S. A. 100, 13190–13195.
Ziebuhr, J., Snijder, E.J., Gorbalenya, A.E., 2000. Virus-encoded proteinases and proteolytic processing in the Nidovirales. J. Gen. Virol. 81, 853–879.